Ab initio simulations of the electrical and optical properties of shock-compressed SiO_2

Yann Laudernet* and Jean Clérouin
Département de Physique Théorique et Appliquée, CEA/DAM Île-de-France, Boîte Postale12, 91680 Bruyères-le-Châtel Cedex, France

Stéphane Mazevet
Theoretical Division, Los Alamos National Laboratory, Los Alamos, New Mexico 87545, USA
(Received 15 December 2003; revised manuscript received 10 May 2004; published 21 October 2004)

We calculate the optical properties of shock-compressed silica up to a pressure of 1200 GPa using *ab initio* molecular-dynamics simulations. The calculations show a significant rise in conductivity and reflectivity as both the pressure and temperature increase. This smooth increase in reflectivity up to a pressure of 500 GPa as well as the saturation value of about 35% given by the simulations are in near perfect agreement with recent shock compression measurements. The constituency analysis performed suggests that this increase in both conductivity and reflectivity can be attributed to the dissociation of molecular systems in the fluid.

DOI: 10.1103/PhysRevB.70.165108 PACS number(s): 78.20.Ci, 31.15.Ar, 62.50.+p

I. INTRODUCTION

Due to its significant abundance in the earth mantle, the behavior of silica, SiO_2, under high pressure has been extensively studied, both theoretically and experimentally, over the past decades. Up to now, however, these studies have mainly focused on the characterization of the different allotropic phases, α-quartz, cristollabite, and stishovite[1,2] which are found for the solid state near room temperature (300 K) and pressures generally below 1 Mbar (1 Mbar=100 GPa). Despite significant progress in our understanding of the behavior of silica in this regime, little is known, however, on its various physical properties for pressures and temperatures above, respectively, 100 GPa and 5000 K.

In the present paper, we focus on the description of the electrical and optical properties of silica for pressures ranging from 100 to 1200 GPa and corresponding temperatures which span from 5000 to 90 000 K. This study is motivated by recent measurements of the Al_2O_3, LiF,[3] and SiO_2 (Ref. 4) reflectivities along the principal Hugoniot using shock compression techniques. These measurements show a significant increase in reflectivity for these three systems, reaching between 20% and 50% at the highest pressures. This smooth rise in reflectivity generally signals a transition from an insulator to a metallic state. At normal conditions, these three crystals present a significant band gap of about 10 eV. The increase in reflectivity observed experimentally has been modeled for LiF and Al_2O_3 as the combined effect of pressure-induced gap closure and thermal excitation resulting from the increase of both pressure and temperature characteristics of shocked experiments.[3] Despite this attempt, the mechanism leading to the semiconductor-metal state is still not clear and requires further investigations using *ab initio* approaches.

To this end, we performed quantum molecular-dynamics (QMD) simulations of shock-compressed silica for conditions corresponding to these recent measurements along the principal Hugoniot. QMD simulations, where the electrons receive a fully quantum-mechanical treatment within the framework of density-functional theory (DFT), have proven to give a reliable description of the solid and liquid properties of silicate up to a pressure of 100 GPa.[5–7] QMD simulations have also been successfully applied to the description of various atomic and molecular fluids and have shown to be well suited to calculate the dynamical, electrical, and optical properties of various systems for conditions met in shock experiments.[8–14] For shocked silica, we find, as for two other systems hydrogen and nitrogen, that the steady rise in conductivity and reflectivity at pressures above 100 GPa can be associated with the continuous dissociation of the molecular fluid. In this regime, and in contrast to the assumption used for the modeling of the LiF and Al_2O_3 reflectivities,[3] the frequency dependent QMD conductivities do not exhibit a Drude-like behavior. This suggests that a nonideal metallic state is reached for SiO_2, even at the highest pressures where measurements were performed. Finally, these findings and the accuracy of the method at describing the properties of SiO_2 in this regime are corroborated by the remarkable agreement between the QMD and experimental reflectivities above 100 GPa.

II. SIMULATION METHOD

In the present application, *ab initio* molecular-dynamics trajectories were generated using the Vienna Ab Initio Simulation Package (VASP) plane-wave code developed at the Technical University of Vienna.[15] Within this package, the electron-ion interactions can be described by either Vanderbilt ultrasoft (US) pseudopotentials[16] or projector augmented wave (PAW) potentials.[17] The exchange correlation term can be treated within the local-density approximation (LDA) or the generalized gradient approximation (GGA) as parametrized by Perdew and Wang.[18]

We tested the different functionals and potentials available by calculating the α-quartz properties at 0 K (cold curve) and 300 K. As noticed by Hamann,[19] the volume dependence of the total energy of α-quartz in the solid phase at 0 K shows that the PAW-LDA calculation gives the closest results to the experimental volume (37.71 $Å^3$). The GGA calculations, US and PAW, both predict higher volumes. The

band structure of α-quartz computed in the LDA approximation agrees very well with previous calculations,[20] showing at the Γ point a direct gap of 5.5 eV and an indirect M-Γ gap of 7.5 eV, compared with the experimental one of 9–9.5 eV (see Ref. 21 and references therein). Accordingly, our computed optical properties will be shifted by 1.8–2 eV toward lower energies when compared to the experimental results. We further note that in this case, *GW* calculations [22] overcorrect the LDA band gaps. In light of these findings, we further calculated the optical properties of α-quartz at 300 K using the PAW-LDA approach.

For both the solid and shocked states investigated in the present work, we follow the Kubo-Greenwood formulation [23,24] to calculate the optical conductivity (atomic units):

$$\sigma(\omega) = \frac{2\pi}{3\omega}\frac{1}{\Omega}\sum_{\mathbf{k}} W(\mathbf{k}) \sum_{n,m,\alpha} (f_n^{\mathbf{k}} - f_m^{\mathbf{k}})|\langle \psi_n^{\mathbf{k}}|\nabla_\alpha|\psi_m^{\mathbf{k}}\rangle|^2 \times \delta(E_m^{\mathbf{k}} - E_n^{\mathbf{k}} - \hbar\omega). \quad (1)$$

In Eq. (1), ω is the frequency, ψ_n and E_n are the electronic eigenstates and eigenvalues for the electronic band n at a given $\mathbf{k}$ point in the Brillouin zone, $W(\mathbf{k})$ is the $\mathbf{k}$-point weight in the Brillouin zone using the Monkhorst-Pack scheme, and f_n is the Fermi distribution function. Finally, the Kubo-Greenwood formulation is applied using the all-electron PAW potential which does not require the correction term related to the nonlocality of the pseudopotential that would be needed if US pseudopotentials were used.[10,17,25]

The δ function is resolved by using a Gaussian regularization.[8,10] The dc electrical conductivity σ_{dc} is obtained by extrapolating the low-frequency optical conductivity to $\omega=0$. The eigenstates and eigenvalues used in the present application are solutions of the Kohn-Sham equations and are thus computed within the local-density approximation. For systems in an arbitrary medium, the reflectivity $r(\omega)$ is defined as

$$r(\omega) = \frac{[n_0(\omega) - n(\omega)]^2 + [k_0(\omega) - k(\omega)]^2}{[n_0(\omega) + n(\omega)]^2 + [k_0(\omega) + k(\omega)]^2}, \quad (2)$$

where the real part $n(\omega)$ and the imaginary part $k(\omega)$ of the index of refraction are related to the dielectric function as

$$\epsilon(\omega) = \epsilon_1(\omega) + i\epsilon_2(\omega) = [n(\omega) + ik(\omega)]^2. \quad (3)$$

$n_0(\omega)$ and $k_0(\omega)$ define the indices of refraction of the surrounding medium. The dielectric function itself follows from the real and imaginary parts of the conductivity as

$$\epsilon_1(\omega) = 1 - \frac{4\pi}{\omega}\sigma_2(\omega), \quad \epsilon_2(\omega) = -\frac{4\pi}{\omega}\sigma(\omega), \quad (4)$$

where the imaginary part of the electrical conductivity arises from the application of the Kramer-Kronig relation

$$\sigma_2(\omega) = -\frac{2}{\pi}P\int \frac{\sigma(\nu)\omega}{(\nu^2 - \omega^2)}d\nu, \quad (5)$$

where P stands for the principal value of the integral.

The hot solid phase of α-quartz (300 K) was simulated using 24 molecules (eight elementary cells) equilibrated for a total time of 4 ps (8000 time steps of 0.5 fs) using a micro-canonical simulation. The optical conductivity and reflectivity were calculated at ten independent configurations using a finer Brillouin-zone sampling and an increased number of bands. The result of the calculation is shown in Fig. 1 and compared with the self-consistent orthogonalized linear combination of atomic orbitals (SCOLCAO) calculations of Xu (Ref. 20) and the experimental data of Philipp.[1,2] Figure 1(a) shows that the first two maxima at 10.1 eV and 11.3 eV are not reproduced by either our PAW-LDA or the SCOLCAO calculations. These maxima have been recently attributed to excitonic effects[22] which are not included in our DFT approach. In agreement with the band-structure calculation, we notice that the onset of the conductivity is shifted by 2 eV to lower energies when compared to the experimental results. In contrast, the optical reflectivity shown in Figure 1(b) reproduces the trend of the experimental curve and yields values at 1 and 2 eV, corresponding to laser frequencies ω and 2ω, in excellent agreement with the experimental values. The reflectivity shown in Figure 1(b) is calculated for a system in vacuum where $n_0(\omega)=1$ and $k_0(\omega)=0$ in Eq. (2). Based on the overall satisfactory description of the physical properties of α-quartz using a PAW-LDA approach, we choose to simulate the electrical and optical properties of compressed silica under the same conditions.

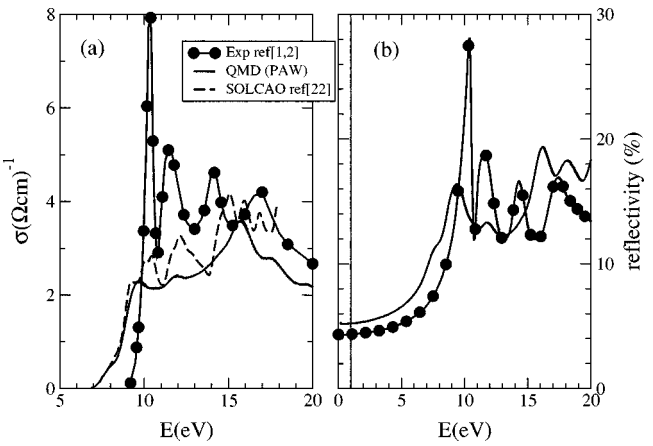

FIG. 1. (a) Optical conductivity vs energy for α-quartz at 300 K. (b) Reflectivity vs energy for α-quartz at 300 K. The full line represents QMD results and the line with full circles the experimental data of Philipp (Refs. 1 and 2).

III. RESULTS

Points along the principal Hugoniot of silica were calculated using 8–54 molecules in the simulation cell. Due to the Fermi distribution, simulations performed at the highest temperatures require to consider a larger number of bands. As the computational time involved increases with the number of bands included in the calculation, the number of particles used needs to be reduced to keep the calculation feasible. As such, we used ten bands for each SiO_2 molecule at $T=7700$ K and 64 at $T=88\,000$ K. For the calculation of the optical properties, the number of bands needs to be further increased to allow for the high-energy transitions and pro-

TABLE I. Comparison between the SESAME and QMD thermodynamical quantities, respectively, T_{eos}, P_{eos} and T_{QMD}, P_{QMD} at a given density ρ_{eos}. The experimental pressures are such that $P_{expt}=P_{eos}$. Also indicated, the number of bands used for each SiO_2 molecule for the trajectory, N_{bands}^{sim}, and the optical calculations, N_{bands}^{opt}. N_{mol} is the number of molecules used in the simulation cell.

P_{expt} (GPa)	ρ_{eos} (g/cm^3)	T_{eos} (K)	P_{QMD} (GPa)	T_{QMD} (K)	N_{mol}	N_{bands}^{sim}	N_{bands}^{opt}	**r** $@\omega_2$
100	4.71	7700	110	8000	54	10	22	0.09
200	5.04	16000	220	16400	16	16	62	0.22
500	5.83	38700	520	40000	16	28	75	0.34
1000	6.57	75800	1020	72100	8	56	98	0.39
1200	6.78	88850	1230	86000	8	64	100	0.39

vide converged optical conductivities. The number of bands used for each condition is given in Table I.

The final-state conditions satisfying the Rankine-Hugoniot relation[26] for fused silica were deduced with the help of the SESAME library[27] as follows. For a given experimental pressure, P_{expt}, a simulation was performed at a corresponding density ρ_{eos} and temperature, T_{eos}, as given by the SESAME equation of state[27] (see Table I). After equilibration and thermalization at T_{eos}, a microcanonical simulation was performed and thermodynamic quantities (P,T,E) averaged. The resulting pressure P_{QMD} was found to be in good agreement (with an uncertainty of 10%) with the SESAME Hugoniot pressure, indicating that the two equations of states (EOS) are consistent. We further tested the validity of accounting for the outer-shell electrons only, 4 and 6 electrons per atom for, respectively, silicon and oxygen, when using the PAW-LDA potentials. A rough estimation of the ionization fraction using the More model[28] yields 3.8 and 3.2 free electrons per atom for, respectively, Si and O at 80 000 K and 1000 GPa which suggests that the potentials used are appropriate. The validity of this assumption is also confirmed by a comparison between the mean sphere and the cutoff radii used in the potentials. This also indicates that simulations performed at higher temperatures and/or pressures than presented here would require the inclusion of inner-shell electrons within the PAW potentials.

From the calculated trajectories, evenly spaced configurations were used to obtain the optical conductivities as described in the preceding section. We show in Fig. 2 the behavior of the optical conductivity as a function of frequency for five temperature-density points representative of the pressure range accessed experimentally (see Table I). We first notice that the structure seen for the optical conductivity of α-quartz at 300 K has disappeared and only a broad maximum remains for all the density-temperature points. In addition, and even at the highest pressure, the behavior of $\sigma(\omega)$ is still not Drude-like and shows a clear maximum at frequencies around 15 eV. Figure 2 also shows that the dc conductivity steadily rises with increase in temperature and pressure up to 500 GPa as is expected for a thermally activated process. Interestingly, the conductivity saturates beyond 500 GPa. The conductivities at 1000 GPa and 1200 GPa are rather close together despite a significant increase in temperature of about 13 000 K.

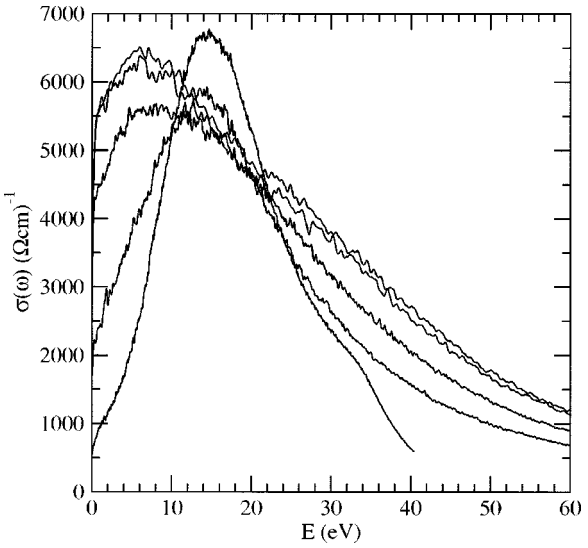

FIG. 2. Optical conductivity vs energy for, from bottom to top, 100, 200, 500, 1000, and 1200 GPa. Corresponding temperatures and pressures are in Table I.

To shed some lights on the mechanism responsible for this behavior, we show, in Fig. 3, the variation of the silicon-oxygen pair correlation function $g_{Si\text{-}O}(r)$ along the principal Hugoniot. At the lowest pressure, $P=100$ GPa, the pair correlation function $g_{Si\text{-}O}(r)$ exhibits a sharp maximum at around $1.5a_B$. This shape clearly indicates that the fluid is mostly in a molecular state, with some dynamically broken bonds. At this pressure, the dc conductivity is rather small and on the order of 700 $(\Omega\ \mathrm{cm})^{-1}$. As the pressure increases, Fig. 3 shows that the maximum clearly noticeable at 100 GPa has significantly declined at 500 GPa. In the meantime, the dc conductivity, shown in Fig. 2, sharply increased to about 4500 $(\Omega\ \mathrm{cm})^{-1}$ at this pressure. At 500 GPa and beyond, the silicon-oxygen pair-correlation function is representative of an atomic fluid indicating that the SiO_2 molecules have almost completely dissociated. Accordingly, the dc conductivities shown in Fig. 3 increase only slightly in this pressure range and reach a plateau at around 5500 $(\Omega\ \mathrm{cm})^{-1}$.

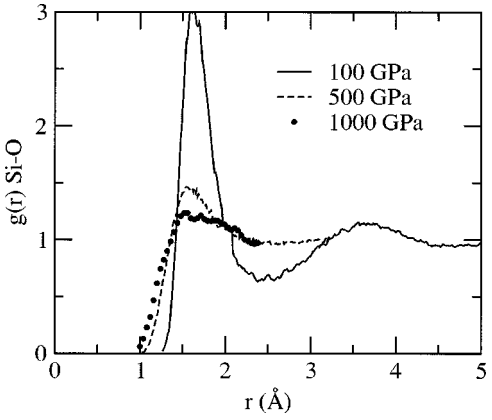

FIG. 3. Pair correlation function $g(r)$Si-O along the principal Hugoniot.

This analysis suggests that a model based on thermally activated processes (TAP) of electrons across a band gap, reduced by the effect of increased pressure, needs to account for the dissociation of the various molecular species present in the media. This direct correlation between the increase in conductivity and the dissociation of molecular systems has already been noticed for other shocked molecular fluids such as hydrogen and nitrogen.[8,13] The result found here for a more complex system, SiO_2, indicates that this correlation is rather generic and characteristic of the behavior of shock-compressed molecular fluids.

To quantify the effect of thermally activated processes on the conductivity, we performed conductivity calculations with zero electronic temperature to eliminate the smearing of the Fermi-Dirac distribution. At 500 GPa, we found no significant differences between the zero and finite temperature calculations. At lower pressure, 100 GPa, we observed a slight divergence at very low frequency. This divergence can be traced back to the finite occupation factor of 2 divided by a vanishing frequency in Eq. (1). This suggests that TAP are negligible in this regime, as confirmed by the inspection of the density of states which shows a closure of the band gap beyond 100 GPa.

In Fig. 4, we compare the variation, as a function of pressure, of the QMD reflectivity at a frequency of $\omega_2 = 532$ nm with the experimental measurements. As the experimental setup is such that the reflectivity is measured at the shock front and through the unshocked media,[3] we choose in Eq. (2) $n_0(\omega_2) = 1.460\,71$ and $k_0(\omega_2) = 0$.[1] The statistical uncertainty on the reflectivity was estimated by choosing 50 samples along the trajectory for the case corresponding to a density of 5.04 g/cm^3 and by plotting the instantaneous values of the reflectivity versus pressure. The standard deviation leads to an estimation of the error bars of about 5% for the reflectivity and 8 GPa for the pressure. Figure 4 shows that, as for the electrical conductivity, the reflectivity saturates once the fluid has dissociated, for pressures of 500 GPa and above. Both the value reached by the reflectivity, about 35%, and the pressure range where this saturation occurs are in perfect agreement with the experimental measurements. This agreement between the measurements and the QMD calculations at 500 GPa and above carries over to lower pressures with the exception of the lowest point at 100 GPa. At 100 GPa, the reflectivity calculated is twice the measured value. We attribute this discrepancy to the well-known underestimation of the vanishing band gap by DFT-LDA methods that was illustrated in the preceding section for α-quartz.

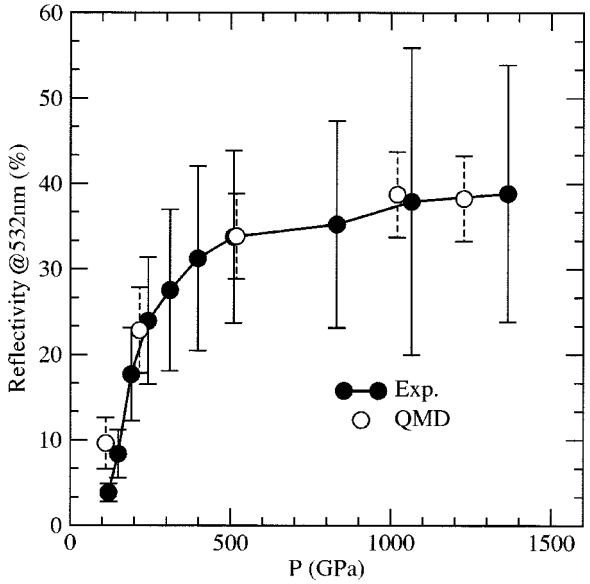

FIG. 4. Reflectivity vs pressure along the principal Hugoniot. Full points are experimental results of Celliers (Ref. 4).

IV. CONCLUSION

We used QMD simulations to calculate the electrical and optical properties of silica along the principal Hugoniot. Despite the well-known underestimation of the band gap by DFT-LDA methods, we show that the method provides a satisfactory description of the variation of reflectivity as a function of pressure in the dense fluid regime. In contrast to assumptions recently used to model this effect, we find that the frequency-dependent conductivity does not show a Drude-like behavior up to 1200 GPa. Finally, we show that the behavior of both the reflectivity and dc conductivity as a function of pressure is directly related to the continuous dissociation of molecular systems along the principal Hugoniot.

ACKNOWLEDGMENTS

We thank G. Collins, D. Hicks, J. Eggert, and P. Celliers for many fruitful discussions and for providing their data prior to publication. M. Knudson, M. Desjarlais, and P. Celliers are also gratefully acknowledged for stimulating discussions during the Cecam organized in Lyon in July 2003. This work was performed under the auspices of an agreement between CEA/DAM and NNSA/DP on cooperation on fundamental science.

*Electronic address: yann.laudernet@cea.fr

[1] H. R. Philipp, J. Phys. Chem. Solids **32**, 1935 (1971).
[2] H. R. Philipp, J. Non-Cryst. Solids **8–10**, 627 (1972).
[3] D. G. Hicks, P. M. Celliers, G. W. Collins, J. H. Eggert, and S. J. Moon, Phys. Rev. Lett. **91**, 035502 (2003).
[4] P. M. Celliers (unpublished).
[5] J. Sarnthein, A. Pasquarello, and R. Car, Phys. Rev. Lett. **74**, 4682 (1995).
[6] M. Benoit, S. Ispas, and M. E. Tuckerman, Phys. Rev. B **64**, 224205 (2001).
[7] A. Trave, P. Tangney, S. Scandolo, A. Pasquarello, and R. Car, Phys. Rev. Lett. **89**, 245504 (2002).
[8] L. A. Collins, S. R. Bickham, J. D. Kress, S. Mazevet, T. J. Lenosky, N. J. Troullier, and W. Windl, Phys. Rev. B **63**,

184110 (2001).
[9] V. Recoules, P. Renaudin, J. Clérouin, P. Noiret, and G. Zérah, Phys. Rev. E **66**, 056412 (2002).
[10] M. P. Desjarlais, J. D. Kress, and L. A. Collins, Phys. Rev. E **66**, 025401 (2002).
[11] V. Recoules, J. Clérouin, P. Renaudin, P. Noiret, and G. Zérah, J. Phys. A **36**, 6033 (2003).
[12] J. Clérouin, P. Renaudin, V. Recoules, P. Noiret, and G. Zérah, Contrib. Plasma Phys. **43**, 269 (2003).
[13] S. Mazevet, J. D. Kress, L. A. Collins, and P. Blottiau, Phys. Rev. B **67**, 054201 (2003).
[14] S. Mazevet, L. A. Collins, N. H. Magee, J. D. Kress, and J. J. Keady, Astron. Astrophys. **405**, 5 (2003).
[15] G. Kresse and J. Hafner, Phys. Rev. B **47**, 558 (1993).
[16] D. Vanderbilt, Phys. Rev. B **41**, 7892 (1990).
[17] G. Kresse and D. Joubert, Phys. Rev. B **59**, 1758 (1999).
[18] J. P. Perdew, *Electronic Structure of Solids* (Akademie Verlag, Berlin, 1991).
[19] D. R. Hamann, Phys. Rev. Lett. **76**, 660 (1996).
[20] Y. N. Xu and W. Y. Ching, Phys. Rev. B **44**, 11 048 (1991).
[21] Z. A. Weinberg, G. W. Rubloff, and E. Bassous, Phys. Rev. B **19**, 3107 (1979).
[22] E. K. Chang, M. Rohlfing, and S. G. Louie, Phys. Rev. Lett. **85**, 2613 (2000).
[23] R. Kubo, J. Phys. Soc. Jpn. **12**, 570 (1957).
[24] D. A. Greenwood, Proc. Phys. Soc. Jpn. **71**, 585 (1958).
[25] P. E. Blochl, Phys. Rev. B **50**, 17 953 (1994).
[26] Y. Zeldovich and Y. Raizer, *Physics of Shock Waves and High-Temperature Hydrodynamic Phenomena* (Academic Press, New York, 1966).
[27] The Los Alamos National Laboratory, Report No. LA-UR-92-3407.
[28] R. M. More, Adv. At. Mol. Phys. **21**, 305 (1985). The More model is based on a finite temperature Thomas-Fermi calculation of the electronic density at the edge of the Wigner-Seitz cell.